TABLE 4. FUNCTIONAL CLASSIFICATION OF KNOWN GENES DOWN-REGULATED AFTER TBI (CONT'D)

Gene name	*Accession number*	*Fold change*
X-linked nuclear protein	AA571771	2.2
Peroxisome proliferative activated receptor, gamma, coactivator 1	AI552694	2.2
Zinc finger protein 37	AA388202	2.1
Zinc finger protein 90	AA517408	2.1
Splicing factor, arginine/serine-rich 5 (SRp40, HRS)	AI120315	2.1
Cathepsin S	AA146437	2.0
Cathepsin L	AA619763	2.0
Carbonic anhydrase 5b, mitochondrial	AA270290	2.0
Heat shock protein, 60 kDa	AA444576	2.0
Nuclear receptor coactivator 4	AA619964	2.0
Zinc finger protein 46	AA269904	2.0
E4F transcription factor 1	AI324466	2.0
Membrane		
ATP synthase, H+ transporting, mitochondrial F1 complex, alpha subunit, isoform 1	AA739359	3.1
ATPase, H+ transporting, lysosomal (vacuolar proton pump), alpha 70 kDa, isoform	AA068612	2.7
Myelin basic protein expression factor 2, repressor	W83960	2.5
Eph receptor A4	AI325333	2.4
Integral membrane protein 2	AA387218	2.4
Integrin alpha 4 (Cd49d)	AA152636	2.3
GPI-anchored membrane protein 1	AA450851	2.3
Inositol 1,4,5-triphosphate receptor 1	AA444527	2.1
Very low density lipoprotein receptor	AA020307	2.1
Gap junction membrane channel protein alpha 1	AA738914	2.0
Cytoskeleton		
Kinesin heavy chain member 2	AA241771	3.0
Alpha-spectrin 1, erythroid	AA116814	2.1
Kinesin family member 21A	AI390275	2.1
Adhesion and molecular recognition		
Integrin alpha 4 (Cd49d)	AA152636	2.3
Activated leukocyte cell adhesion molecule	AA265329	2.0
Others		
Solute carrier family 1, member 2	AA397107	4.5
Protein kinase, cAMP dependent, catalytic, beta	AA683704	3.5
DEAD (aspartate-glutamate-alanine-aspartate) box polypeptide 5	AA414411	3.1
Adenomatosis polyposis coli	AA855420	3.0
Maternally expressed gene 3	W97303	3.0
Transferrin receptor	AA413490	3.0
Neural precursor cell expressed, developmentally down-regulated gene 4	AA067727	2.9
Eukaryotic translation initiation factor 4, gamma 2	AA437871	2.8
Guanine deaminase	AA959127	2.8
Maternal embryonic message 3	AW209270	2.7
DNA segment, Chr 6, ERATO Doi 109, expressed	AA420359	2.5
Transforming growth factor alpha regulated gene 4	AA450513	2.5
Eukaryotic translation initiation factor 4A2	AA638385	2.4
MORF-related gene X	AA545943	2.4
Tetratricopeptide repeat domain	AA881399	2.4
Complement receptor 2	AA208784	2.3
Cullin 3	AA547180	2.3
Heat shock protein, 86 kDa 1	AA529377	2.3
Tial1 cytotoxic granule-associated RNA-binding protein-like 1	W41637	2.3
Tumor rejection antigen gp96	AA469667	2.3
Unc5 homolog (C. elegans) 3	AI047720	2.3
Dystrobrevin alpha	AA386892	2.2

TABLE 4. FUNCTIONAL CLASSIFICATION OF KNOWN GENES DOWN-REGULATED AFTER TBI (CONT'D)

Gene name	*Accession number*	*Fold change*
Platelet-activating factor acetylhydrolase, isoform 1b, beta 1 subunit	AA067153	2.2
RAD21 homolog (S. pombe)	AI154347	2.2
ADP-ribosylation-like factor 6 interacting protein 2	AA414388	2.1
cDNA sequence AB017026	AA414046	2.1
Farnesyltransferase, CAAX box, alpha	AA415472	2.1
Glia maturation factor, beta	AA575789	2.1
Hippocampus abundant gene transcript 1	AA414014	2.1
Integrin-associated protein	AA204140	2.1
Itchy	AA105796	2.1
Molybdenum cofactor synthesis 2	AI592114	2.1
CAMP protein (Camp)	AI594093	2.1
Pantophysin	AI325652	2.1
Purkinje cell protein 1	AA547170	2.1
Sarcoglycan, beta (43 kD dystrophin-associated glycoprotein)	W61688	2.1
SEC23A (S. cerevisiae)	AA867862	2.1
Septin 3	AI605734	2.1
Solute carrier family 3, member 1	AI385484	2.1
T-complex testis expressed 1	AI596504	2.1
WD40 protein Ciao1	AA117997	2.1
ADP-ribosylation-like factor 6 interacting protein	AA606940	2.0
Bcl2-interacting killer/like	AA726901	2.0
Chromobox homolog 3 (Drosophila HP1 gamma)	AA547637	2.0
Eukaryotic translation elongation factor 1 alpha 1	AA212150	2.0
Eukaryotic translation initiation factor 1A	AA422861	2.0
Neurogranin (protein kinase C substrate, RC3)	AA050507	2.0
p21 (CDKN1A)-activated kinase 3	AA387195	2.0
Ring finger protein 11	AA437704	2.0
Syntaxin 7	AA111166	2.0
Synuclein, alpha	AI510034	2.0
Tight junction protein 1	AW210329	2.0
Tumor susceptibility gene 101	AA065752	2.0

Accession numbers listed are GenBank accession numbers.

DISCUSSION

Our present data indicate that TBI influences cells in remote areas such as the SVZ and DG. Proliferation, migration, and neuronal differentiation in the SVZ have been reported in a brain ischemia model (Arvidsson et al., 2002; Jin et al., 2001; Nakatomi et al., 2002), suggesting that NSCs participate in self-repair after brain damage causes neuronal and glial cell death (Pende et al., 1997). However, NSCs do not appear to contribute to effective neural regeneration after TBI; we did not observe BrdU-labeled neurons even at 14 days after brain injury (data not shown). Proliferating cells might die or become glial cells in our mechanical injury model. To develop new strategies to manipulate NSCs for regeneration after TBI, it is necessary to understand the molecular mechanisms that regulate proliferation, migration, and differentiation of NSCs after TBI. Therefore, we used cDNA microarrays to examine changes in gene expression after TBI, expecting that they might provide useful information regarding the microenvironment around NSCs.

Recent progress in cDNA microarray technology has enabled simultaneous analysis of thousands of genes associated with specific biological events. This technique has been used to investigate aging, inflammation, tumor metastasis, seizures, and neurodegenerative disorders. Several groups have used this technique to investigate genetic mechanisms regulating the function and differentiation of NSCs in the CNS. Geschwind et al. (2001) used representational difference analysis and microarray technology coupled with anatomical screening to char-

TABLE 5. EXPRESSED SEQUENCE TAGS DOWN-REGULATED AFTER TBI

Accession number	*Fold change*	*Accession number*	*Fold change*	*Accession number*	*Fold change*
AI592051	4.0	AA422260	2.4	AA543485	2.1
W82301	3.4	AA473948	2.4	AA684094	2.1
AA275241	3.3	AA691036	2.4	AA727007	2.1
AI227494	3.2	AA693177	2.4	AA762870	2.1
AA028359	3.1	AI596293	2.4	AA789551	2.1
AA619844	3.1	AA060880	2.3	AA794176	2.1
W36425	3.1	AA474047	2.3	AI390606	2.1
AA619869	3.0	AI120239	2.3	AI464905	2.1
AA261404	2.9	AI592148	2.3	AI536399	2.1
AA545397	2.9	AI597424	2.3	AI592084	2.1
AA596555	2.9	AI643212	2.3	AI614942	2.1
AA762383	2.9	AA000282	2.2	AW210318	2.1
AI892497	2.9	AA185228	2.2	AA063757	2.0
AA437919	2.8	AA466153	2.2	AA116742	2.0
AA546964	2.8	AA518515	2.2	AA254541	2.0
W09948	2.8	AA638578	2.2	AA267285	2.0
AI464603	2.7	AA645878	2.2	AA288456	2.0
AA189752	2.6	AI019625	2.2	AA414193	2.0
AA500239	2.6	AI020979	2.2	AA529691	2.0
AA537011	2.6	AI120198	2.2	AA544754	2.0
AI450492	2.6	AI390228	2.2	AA545395	2.0
AI644761	2.6	AI390992	2.2	AA546740	2.0
AI645264	2.6	AI508515	2.2	AA555793	2.0
AA189544	2.5	AI508571	2.2	AA615254	2.0
AA204221	2.5	AI553049	2.2	AA619843	2.0
AA474446	2.5	AI608045	2.2	AA623811	2.0
AA547033	2.5	AA175485	2.1	AA738637	2.0
AA549540	2.5	AA175822	2.1	AA982338	2.0
AA675294	2.5	AA242024	2.1	AI180948	2.0
AA718770	2.5	AA245754	2.1	AI390650	2.0
AA880332	2.5	AA268576	2.1	AI509284	2.0
AI427715	2.5	AA278088	2.1	AI595068	2.0
AI645217	2.5	AA414279	2.1		
AI645230	2.5	AA419710	2.1		
AA068481	2.4	AA444227	2.1		

GenBank accession number and fold change are listed.

acterize gene expression patterns in pluripotent proliferating progenitor cells relative to cells at later stages of differentiation. Luo et al. (2002) used microarrays containing approximately 500 known genes related to cell cycle regulation, apoptosis, growth, and differentiation to assess and compare gene expression in fetal neuroepithelial cells and progenitor cells.

Several microarray studies of CNS injury have also been published. Song et al. (2001) analyzed 1263 genes and found 76 transcripts were differentially expressed at 3 h and/or 24 h after spinal cord injury (SCI). As early as 3 h after SCI they observed increased expression of genes associated with transcription, inflammation, and neurotransmitter dysfunction and found decreased expression of genes associated with ionic imbalance and cytoskeletal damage and a disruption of protein phosphorylation and second-messenger signaling. By 24 h after SCI, in addition to these effects, endogenous attempts to regenerate and stabilize function of the injured spinal cord begin.

Matzilevich et al. (2002) examined expression of 8,800 genes in the hippocampus of TBI rats by microarray. They provided comprehensive information on 524 differentially expressed genes in the hippocampus at 3 h and/or 24 h following TBI. Their data indicated that, as early as 3 h after TBI, expression of genes associated with the cell cycle, glucose metabolism, reactive oxygen species metabolism, and inflammation is increased. By

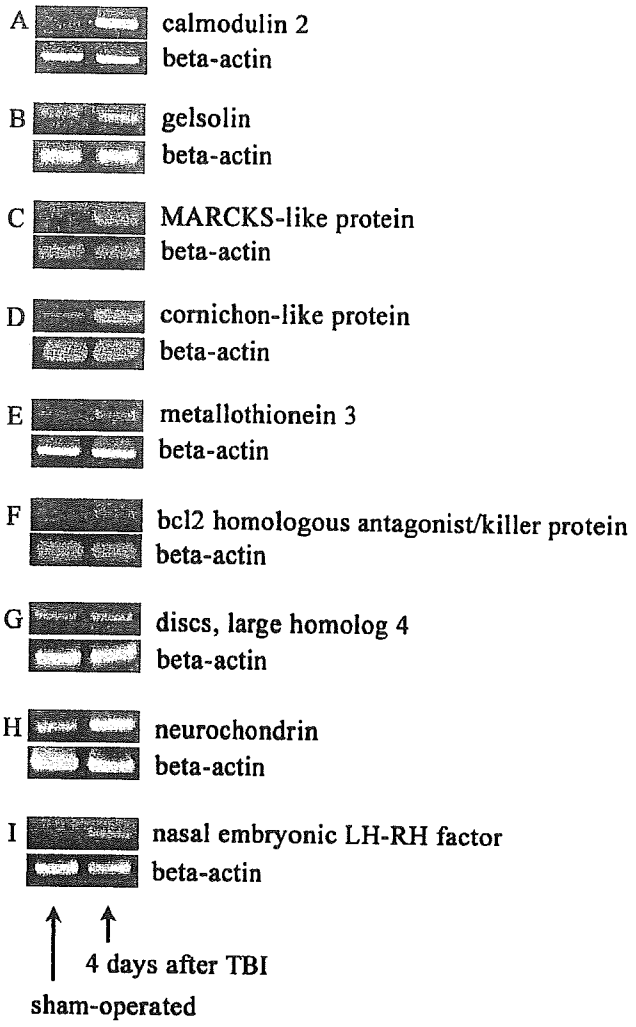

FIG. 3. Differential expression of mRNA as assessed by RT-PCR. Samples were taken from the SVZ of sham-operated rats (left side) and from the ipsilateral SVZ of injured rats 4 days after TBI (right side).

24 h, these transcripts had returned to basal levels, and the expression of genes encoding membrane and cytoskeletal proteins was altered. Levels of genes related to neurotransmitters and calcium signaling were also decreased. These data are similar to those of Song et al. (2001).

Jenkins et al. (2002) examined global changes in hippocampal proteins in immature 17-day-old rats 24 h after TBI. They observed increased levels of glucose metabolism, reactive oxygen species metabolism, and cytosolic chaperone/stress proteins, and decreased levels of cytoskeletal, nuclear, and membrane proteins.

Our results differ from those of previous reports. We analyzed gene expression in an area remote from the site of TBI, the SVZ, because we were interested in mechanisms regulating NSCs in remote sites. We did not observe significant changes in expression of genes encoding structural proteins, such as cytoskeletal proteins, membrane proteins, and ion channels. We analyzed gene expression at 4 days after TBI to focus on the regenerative stage after injury. Therefore, little change in the expression of inflammatory genes and immediate early genes was observed. In contrast, we observed increased expression of genes associated with cell proliferation and differentiation, such as cornichon-like (Cnil) and cystatin C. Cnil is a homolog of *Drosophila* cornichon, which is involved in epidermal growth factor receptor (EGFR) signaling during development (Roth et al., 1995). Cystatin C is a cofactor of fibroblast growth factor 2 (FGF2), which is required when FGF2-responsive neural stem cells proliferate (Taupin et al., 2000). EGF and FGF2 have been reported to cause proliferation and differentiation of NSCs in the SVZ of adult rodents (Kuhn et al., 1997), and they also may have important roles in the SVZ after TBI.

In the present study, the number of BrdU-positive cells increased in the SVZ after TBI, but the number of nestin-positive cells did not increase. These findings suggest that NSCs proliferate but soon die or differentiate into glial, not neuronal, cells. Therefore, we hypothesized that genes related to apoptosis and differentiation into neuronal/glial lineages would be altered. However, we identified only a few known genes associated with apoptosis and neuronal/glial fate. Further studies of the roles of differentially expressed genes in regulating NSCs are needed.

Possible Functional Implication of Altered Gene Expression

Levels of Calm2 mRNA were increased in the SVZ after TBI. Calmodulin is involved in calcium signaling in eukaryotic cells and binds calcium ions to form a Ca^{2+}/calmodulin complex. This complex then binds and inactivates autoinhibitory domains of protein kinases, including myosin light chain kinase, Ca^{2+}/calmodulin-dependent kinases, protein kinase C (PKC), and Ca^{2+}/calmodulin-dependent adenylate cyclase (Arbuzova et al., 2002; Means, 1994), and regulates cellular proliferation and differentiation. In particular, Ca^{2+}/calmodulin-dependent kinases have been shown to play essential roles in the G1 to S phase transition in the cell cycle, and many cellular regulatory cascades rely on CaM for their function (Endres et al., 1999). Therefore, Calm2 may promote cell proliferation in the SVZ after injury.

MLP, which showed increased expression after TBI, is a member of the MARCKS gene family and a major

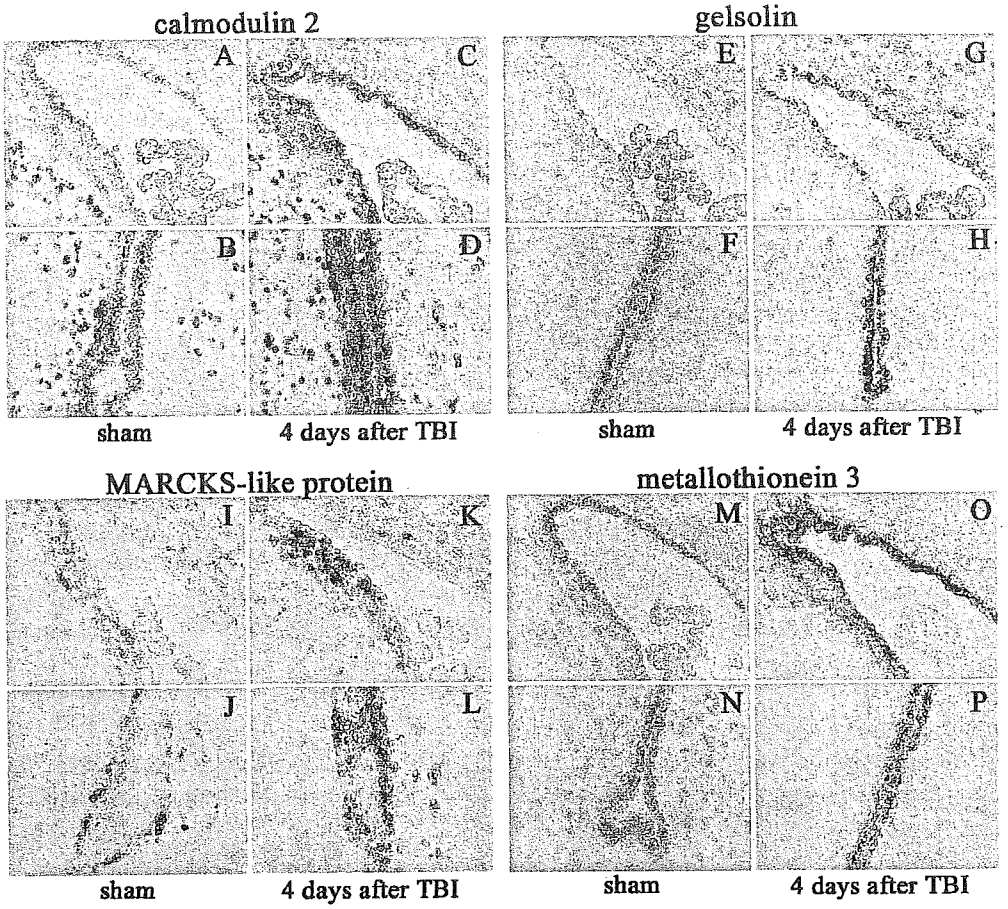

FIG. 4. (**A–D**) *In situ* hybridization analysis of Calm2 mRNA (×200). Expression of Calm2 mRNA was induced predominantly in the cells of the subependymal layer after TBI, although it does not appear to be expressed in ependymal cells (**C,D**). Calm2 mRNA was expressed at low levels in sham-operated rats (**A,B**). (**E–H**) Expression of gelsolin mRNA (×200). Gelsolin mRNA was expressed at high levels in the ependymal and subependymal layers 4 days after TBI (**G,H**), whereas it was expressed at low levels in sham-operated rats (**E,F**). (**I–L**) Expression of MLP mRNA (×200). Expression of MLP mRNA was induced broadly around the ventricular zone after TBI (**K,L**). There were fewer intense signals in the SVZ of sham-operated rats (**I,J**). (**M–P**) Expression of MT-3 mRNA (×200). MT-3 was detected in the ependymal and subependymal layers and was upregulated after TBI (**O,P**), whereas MT-3 was mildly expressed in sham-operated rats (**M,N**). The left panels for all genes are the SVZ of sham-operated rats, and the right panels for all genes are the ipsilateral SVZ of injured rats 4 days after TBI.

substrate of PKC. MARCKS binds the plasma membrane through its N-terminal myristoyl moiety, and the effector domain can translocate reversibly into the cytosol, either through cycles of phosphorylation by PKC and dephosphorylation or through temporary increases in the intracellular calcium concentration leading to activation of CaM. The interaction of PKC and CaM with MARCKS is mutually exclusive. Therefore, MARCKS family proteins are thought to be involved in the crosstalk between PKC and CaM and to regulate diverse cellular functions, including survival, migration, and adhesion (Furukawa et al., 1997). Ca^{2+} also activates the actin-severing protein gelsolin, which mediates dynamic changes in the actin filament network. Thus, gelsolin, which was also upregulated in the present study, acts as an intracellular Ca^{2+} sensor, negatively regulating Ca^{2+} influx and thereby protecting against neuronal dysfunction and death (Hidalgo et al., 2001; Tsuji et al., 1992). Further studies are needed to clarify how the Ca^{2+}/CaM complex is activated in NSCs after TBI.

Metallothionein 3 (MT-3; also known as growth inhibitory factor) is a member of the metallothionein (MT) family. All MT isoforms (MT-1, -2, -3, and -4) have been implicated in nonessential physiological functions, such as zinc and copper metabolism, protection against reactive oxygen species, and adaptation to stress. MT-3 plays

additional roles in neuromodulatory events (Uchida et al., 1991). MT-3 is expressed predominantly within the CNS and is found at low levels in other tissues, although other MTs are widely expressed in all tissues. MT-3 was originally described as a molecule able to inhibit the survival and neurite formation of cortical neurons *in vitro* (Anezaki et al., 1995; Hozumi et al., 1995). Stab wound injury significantly increases MT-3 expression in reactive astrocytes (Hozumi et al., 1996; Hwang et al., 1999; Yuguchi et al., 1997). Brain injury by kainic acid also upregulates MT-3 in reactive astrocytes in the CA3 subfield. MT-3 expression is increased transiently in the ipsilateral cortex at 4 days after cortical ablation of the somatosensory cortex, whereas increased MT-3 expression is increased in the peri-injury site for 2–3 weeks after injury (Yuguchi et al., 1995).

In the present study, expression of MT-3 mRNA was induced in the SVZ but not in areas adjacent to the TBI. However, the function of MT-3 in the SVZ is unknown, and studies of gain or loss of function of MT-3 are needed to address the role of MT-3 under pathological conditions.

In summary, we have described differential gene expression in the SVZ after TBI. Future studies of specific genes will help clarify mechanisms regulating NSCs in the SVZ after brain injury and may help in the development of strategies to regenerate the CNS after damage.

ACKNOWLEDGMENTS

This work was supported by Grants-in-Aid for Scientific Research from the Ministry of Education, Culture, Sports, Science, and Technology of Japan, by grants from the Marine and Fire Insurance Association of Japan, Inc., and by grants for Research on Brain Science from the Ministry of Health, Labour, and Welfare of Japan. We thank Masahiro Ogihara, Yoshinori Ohshima, Hiroomi Ipposhi, and Naoyuki Sato (Kurabo Industries, Ltd.) for participating in this work.

REFERENCES

ALTMAN, J., and DAS, G.D. (1965). Autoradiographic and histological evidence of postnatal hippocampal neurogenesis in rats. J. Comp. Neurol. **124,** 319–335.

ALTMAN, J. (1969). Autoradiographic and histological studies of postnatal neurogenesis. IV. Cell proliferation and migration in the anterior forebrain, with special reference to persisting neurogenesis in the olfactory bulb. J. Comp. Neurol. **137,** 433–457.

ANEZAKI, T., ISHIGURO, H., HOZUMI, I., et al. (1995). Expression of growth inhibitory factor (GIF) in normal and injured rat brains. Neurochem. Int. **27,** 89–94.

ARBUZOVA, A., SCHMITZ, A.A., and VERGERES, G. (2002). Cross-talk unfolded: MARCKS proteins. Biochem. J. **362,** 1–12.

ARVIDSSON, A., COLLIN, T., KIRIK, D., et al. (2002). Neuronal replacement from endogenous precursors in the adult brain after stroke. Nat. Med. **8,** 963–970.

CATTANEO, E., and McKAY, R. (1991). Identifying and manipulating neuronal stem cells. Trends Neurosci. **14,** 338–340.

DASH, P.K., MACH, S.A., and MOORE, A.N. (2001). Enhanced neurogenesis in the rodent hippocampus following traumatic brain injury. J. Neurosci. Res. **63,** 313–319.

DIXON, C.E., CLIFTON, G.L., LIGHTHALL, J.W., et al. (1991). A controlled cortical impact model of traumatic brain injury in the rat. J. Neurosci. Methods **39,** 253–262.

ENDRES, M., FINK, K., ZHU, J., et al. (1999). Neuroprotective effects of gelsolin during murine stroke. J. Clin. Invest. **103,** 347–354.

FURUKAWA, K., FU, W., LI, Y., et al. (1997). The actin-severing protein gelsolin modulates calcium channel and NMDA receptor activities and vulnerability to excitotoxicity in hippocampal neurons. J. Neurosci. **17,** 8178–8186.

GESCHWIND, D.H., OU, J., EASTERDAY, M.C., et al. (2001). A genetic analysis of neural differentiation. Neuron **29,** 325–339.

GOULD, E., and TANAPAT, P. (1997). Lesion-induced proliferation of neuronal progenitors in the dentate gyrus of the adult rat. Neuroscience **80,** 427–436.

GOULD, E., and TANAPAT, P. (1999). Stress and hippocampal neurogenesis. Biol. Psychiatry **46,** 1472–1479.

GOULD, E., REEVES, A.J., GRAZIANO, M.S., et al. (1999). Neurogenesis in the neocortex of adult primates. Science **286,** 548–552.

HIDALGO, J., ASCHNER, M., ZATTA, P., et al. (2001). Roles of the metallothionein family of proteins in the central nervous system. Brain Res. Bull. **55,** 133–145.

HOZUMI, I., INUZUKA, T., HIRAIWA, M., et al. (1995). Changes of growth inhibitory factor after stab wounds in rat brain. Brain Res. **688,** 143–148.

HOZUMI, I., INUZUKA, T., ISHIGURO, H., et al. (1996). Immunoreactivity of growth inhibitory factor in normal rat brain and after stab wounds—an immunocytochemical study using confocal laser scan microscope. Brain Res. **741,** 197–204.

HWANG, S.Y., OH, B., ZHANG, Z., et al. (1999). The mouse cornichon gene family. Dev. Genes Evol. **209,** 120–125.

JENKINS, L.W., PETERS, G.W., DIXON, C.E., et al. (2002). Conventional and functional proteomics using large format two-dimensional gel electrophoresis 24 hours after controlled cortical impact in postnatal day 17 rats. J. Neurotrauma **19,** 715–740.

JIN, K., MINAMI, M., LAN, J.Q., et al. (2001). Neurogenesis in dentate subgranular zone and rostral subventricular zone after focal cerebral ischemia in the rat. Proc. Natl. Acad. Sci. U.S.A. **98,** 4710–4715.

KEMPERMANN, G., KUHN, H.G., and GAGE, F.H. (1997). More hippocampal neurons in adult mice living in an enriched environment. Science **386,** 493–495.

KERNIE, S.G., ERWIN, T.M., and PARADA. L.F. (2001). Brain remodeling due to neuronal and astrocytic proliferation after controlled cortical injury in mice. J. Neurosci. Res. **66,** 317–326.

KUBO, T., YAMASHITA, T., and TOHYAMA, M. (2002). Analysis of genes induced in peripheral nerve after axotomy using cDNA microarrays. J. Neurochem. **83,** 67–79.

KUHN, H.G., WINKLER, J., KEMPERMANN, G., et al. (1997). Epidermal growth factor and fibroblast growth factor–2 have different effects on neural progenitors in adult rat brain. J. Neurosci. **17,** 5820–5829.

LIU, J., SOLWAY, K., MESSING, R.O., et al. (1998). Increased neurogenesis in the dentate gyrus after transient global ischemia in gerbils. J. Neurosci. **18,** 7768–7778.

LOIS, C., and ALVAREZ-BUYLLA, A. (1993). Proliferating subventricular zone cells in the adult mammalian forebrain can differentiate into neurons and glia. Proc. Natl. Acad. Sci. U.S.A. **90,** 2074–2077.

LOIS, C., GARCIA-VCRDUGO, J.M., and ALVAREZ-BUYLLA, A. (1996). Chain migration of neuronal precursors. Science **271,** 978–981.

LUO, Y., CAI, J., LIU, Y., et al. (2002). Microarray analysis of selected genes in neural stem and progenitor cells. J. Neurochem. **83,** 1481–1487.

MAGAVI, S.S., LEAVITT, B.R., and MACKLIS, J.D. (2000). Induction of neurogenesis in the neocortex of adult mice. Nature **405,** 951–955.

MATZILEVICH, D.A., RALL, J.M., MOORE, A.N., et al. (2002). High-density microarray analysis of hippocampal gene expression following experimental brain injury. J. Neurosci. Res. **67,** 646–663.

McKAY, R. (1997). Stem cells in the central nervous system. Science **276,** 66–71.

MEANS, A.R. (1994). Calcium, calmodulin and cell cycle regulation. FEBS Lett. **349,** 1–4.

NAKATOMI, H., KURIU, T., OKABE, S., et al. (2002). Regeneration of hippocampal pyramidal neurons after ischemic brain injury by recruitment of endogenous neural progenitors. Cell **110,** 429–441.

PARENT, J.M., YU, T.W., LEIBOWITZ, R.T., et al. (1997). Dentate granule cell neurogenesis is increased by seizures and contributes to aberrant network reorganization in the adult rat hippocampus. J. Neurosci. **17,** 3727–3738.

PENDE, M., FISHER, T.L., SIMPSON, P.B., et al. (1997). Neurotransmitter- and growth factor-induced cAMP response element binding protein phosphorylation in glial cell progenitors: role of calcium ions, protein kinase C, and mitogen-activated protein kinase/ribosomal S6 kinase pathway. J. Neurosci. **17,** 1291–1301.

ROTH, S., NEUMAN-SILBERBERG, F.S., BARCELO, G., et al. (1995). Cornichon and the EGF receptor signaling process are necessary for both anterior-posterior and dorsal-ventral pattern formation in Drosophila. Cell **16,** 967–978.

SONG, G., CECHVALA, C., RESNICK, D.K., et al. (2001). GeneChip^{R} analysis after acute spinal cord injury in rat. J. Neurochem. **79,** 804–815.

TAUPIN, P., RAY, J., FISCHER, W.H., et al. (2000). FGF-2-responsive neural stem cell proliferation requires CCg, a novel autocrine/paracrine cofactor. Neuron **28,** 385–397.

TSUJI, A., KOBAYASHI, H., UCHIDA, Y., et al. (1992). Molecular cloning of human growth inhibitory factor DNA and its downregulation in Alzheimer's disease. EMBO J. **11,** 4843–4850.

UCHIDA, Y., TAKIO, K., TITANI, K., et al. (1991). The growth inhibitory factor that is deficient in the Alzheimer's disease brain is a 68–amino acid metallothionein-like protein. Neuron **7,** 337–347.

VAN PRAAG, H., KEMPERMANN, G., and GAGE, F.H. (1999). Running increases cell proliferation and neurogenesis in the adult mouse dentate gyrus. Nat. Neurosci. **2,** 266–270.

WEISS, S., REYNOLDS, B.A., VESCOVI, A.L., et al. (1996). Is there a neural stem cell in the mammalian forebrain? Trends Neurosci. **19,** 387–393.

YOSHIMURA, S., TAKAGI, Y., HARADA, J., et al. (2001). FGF-2 regulation of neurogenesis in adult hippocampus after brain injury. Proc. Natl. Acad. Sci. U.S.A. **98,** 5874–5879.

YUGICHI, T., KOHMURA, E., YAMADA, K., et al. (1995). Expression of growth inhibitory factor mRNA following cortical injury in rat. J. Neurotrauma **12,** 299–306.

YUGUCHI, T., KOHMURA, E., SAKAKI, T., et al. (1997). Expression of growth inhibitory factor mRNA after focal ischemia in rat brain. J. Cereb. Blood Flow Metab. **17,** 745–752.

Address reprint requests to:
Kazuhisa Yoshiya, M.D.
Department of Traumatology and
Acute Critical Medicine
Osaka University Graduate School of Medicine
2-2 Yamadaoka
Suita, Osaka 565-0871, Japan

E-mail: yoshiya@hp-emerg.med.osaku-u.ac.jp

The morphological and neurochemical effects of diffuse brain injury on rat central noradrenergic system

Toshiyuki Fujinaka, Eiji Kohmura, Takamichi Yuguchi and Toshiki Yoshimine

Department of Neurosurgery, Osaka University Medical School, Osaka, Japan

The central noradrenergic system is widely distributed throughout the brain and is closely related to spontaneous motility and level of consciousness. The study presented here evaluated the morphological as well as neurochemical effects of diffuse brain injury on the central noradrenergic system in rat. Adult male Sprague–Dawley rats were subjected to impact–acceleration brain injury produced with a weight-drop device. Morphological changes in locus coeruleus (LC) neurons were examined by using immunohistochemistry for dopamine-β-hydroxylase, and norepinephrine (NE) turnover in the cerebral cortex was measured by high performance liquid chromatography with electrochemical detection. The size of LC neurons increased by 11% 24 h after injury but had decreased by 27% seven days after injury. Axons of noradrenergic neurons were swollen 24 h and 48 h after injury but the swelling had dwindled in seven days. NE turnover was significantly reduced seven days after injury and remained at a low level until eight weeks after injury. These results suggest that focal impairment of axonal transport due to diffuse brain injury causes cellular changes in LC and that the neurochemical effect of injury on the central noradrenargic system lasts over an extended period of time. Chronic suppression of NE turnover may explain the sustained behavioral and psychological abnormalites observed in a clinical situation. [Neurol Res 2003; **25**: 35–41]

Key Words: Locus coeruleus; diffuse brain injury; norepinephrine (NE); 3-methoxy-4-hydroxyphenylglycol (MHPG); dopamine-β-hydroxylase

INTRODUCTION

Protracted disturbance of consciousness and lowered motility are the major problems in patients who survive severe head injury. Neuropsychological deficits prevent them from returning to a normal life even if they have physically recovered. Various neurotransmitter pathways in the central nervous systems are likely to be damaged in diffuse brain injury, and alterations in neurotransmitters may be the main cause of psychological and behavioral abnormalities after diffuse brain injury.

The central noradrenergic system, distributed widely throughout the brain, is closely related to changes in activity and level of consciousness in post-traumatic subjects[1–8]. Recent studies suggest that the release and turnover of norepinephrine (NE) are affected by traumatic brain injury, the mode and severity being dependent on various factors such as the type, site and side of injury, time after injury and site of assesment[9–14]. Recent studies have also indicated that central NE facilitates functional recovery after various types of experimental brain injury such as sensorimotor cortex ablation, cerebral contusion or fluid percussion injury[15–21]. In a rat model of local brain injury, NE release and turnover increased during the first few hours and then started to decrease 24 h after injury[13,22,23]. These effects of injury on the central noradrenergic system may play a major role in the disturbance of consciousness and behavioral deficits following diffuse brain injury. In the present study, the effects of diffuse brain injury on the central noradrenergic system were investigated in rats. The morphological changes in the central noradrenergic system were evaluated in the locus coeruleus (LC) neurons and the neurochemical changes were assessed in terms of NE metabolism.

MATERIALS AND METHODS

Diffuse brain injury model

An impact–acceleration injury model was produced according to the method of Marmarou *et al.*[24,25] with modifications. Adult male Sprague–Dawley rats weighing 500–550 g were anesthetized with intraperitoneal chloral hydrate (350 mg kg^{-1}), and an additional injection was administered during the experiment if needed. A midline scalp incision was made and periosteum was reflected to expose the skull between the coronal and lambdoid sutures. A metallic disc 20 mm in diameter and 1.5 mm thick was secured to the exposed skull

Correspondence and reprint requests to: Toshiyuki Fujinaka, MD, Department of Neurosurgery, Osaka University Medical School, 2-2 Yamadaoka, Suita, Osaka 565-0871, Japan. [fujinaka@nsurg.med.osaka-u.ac.jp] Accepted for publication July 2002.

0161-6412/03/010035-07

vertex with cyanoacrylic glue. The animals were then placed in the prone position on a form bed while breathing spontaneously. Impact–acceleration brain injury was achieved with a weight-drop device. A brass weight (450 g) was dropped freely by force of gravity from a height of 1.5 m onto the metallic disc. The rat was moved away immediately following the initial impact to avoid a second insult and then observed for several minutes. After removal of the disc, the scalp was sutured and the rat was returned to its cage (injury group). For the control group, rats were treated as described above except for receiving impact.

All animal experiments were conducted in compliance with the Osaka University Medical School Guidelines for the Care and Use of Laboratory Animals. Animal surgery and the experimental procedure were approved by the Committee for Animal Care and Use, Osaka University Medical School.

Brain fixation and immunohistochemistry

The animals were anesthetized 1, 2, 7, 14, 28, and 56 days after injury and perfused intracardially first with saline and then with 4% paraformaldehyde in 0.1 M phosphate buffer. Four animals each from the injury and control groups were used for each experimental period. The brains were removed and post-fixed with the same fixative for 24 h at 4°C. After immersion in 30% sucrose in 0.01 M phosphate buffered saline (PBS), the brains were embedded in Tissue-Tech and stored at −80°C. Fixed brains were sliced into 12 μm serial coronal sections from 8 mm to 11 mm posterior to the bregma, including the LC, with a freezing microtome and processed for immunohistochemistry.

Immunohistochemistry was used to identify dopamine-β-hydroxylase (DBH) and neurofilaments. Sections were washed in PBS and permeabilized with acetone at −20°C for 10 min, incubated with 0.3% hydrogen peroxide for 30 min to quench intrinsic peroxidase, and washed three times for 5 min each in PBS. Blocking of nonspecific binding was achieved with 2% normal horse serum in a buffer (0.1% Triton X-100 and 5% sucrose in PBS) for 20 min, and sections were finally incubated overnight at 4°C with the primary antibodies. The antibodies used for the immunohistochemical studies were anti dopamine-β-hydroxylase rabbit polyclonal antibody (Eugene Tech International, Ridgefield Park, NJ, USA; diluted 1 : 1000) and anti-68kD-neurofilament mouse monoclonal antibody (Boehringer Mannheim Biochemica, Germany; diluted 1 : 50). The sections were washed in PBS three times for 5 min each, incubated with biotinylated anti-mouse-rabbit IgG (Vectastain Elite ABC Universal Kit, Vector Laboratories, Inc., Burlingame, CA, USA; diluted 1 : 200) for 60 min, and after three 5-min washes in PBS, re-incubated with avidin–biotin peroxydase complex (Vectastain Elite ABC Kit; diluted 1 : 100) for 60 min. Immunolabeled structures were visualized with 0.05% 3,3′-diamino-benzidine tetrahydrochloride (DAB) and 0.01% hydrogen peroxide in PBS. The precipitate formed by DAB was enhanced with 0.8% $NiCl_2$ in PBS. Finally, the sections were washed in water and dehydrated in ethanol for mounting.

Measurement of cellular size

Every fifth serial coronal section immunostained with DBH was assessed to evaluate the changes in cellular size in the LC. The microscopic images of the LC were captured with a digital camera (Fujix HC-300; Fujifilm) mounted on a microscope with 20 objective lens, and stored in a computer. The cross sectional area of each of the stained neurons was measured with the aid of an image-analysis program (Scion Image, Scion Corp., Frederick, MD, USA). Only the stained area containing the nucleus was measured to avoid the cut edge, and measurements were averaged for all sections from one side of the LC and shown as a percentage of control animals. The data were expressed as mean ± SEM values. Statistical differences in the cellular size between the experimental and control groups were assessed by an analysis of variance (ANOVA) with the Newman-Keuls test for intergroup multiple comparisons. Differences were considered to be statistically significant at p-values of 0.05 or less.

Quantitative measurement of brain catecholamines

The tissue levels of NE and 3-methoxy-4-hydroxyphenylglycol (MHPG), the major extracellular metabolite of NE, in the bilateral cerebral cortex were measured by using high performance liquid chromatography with electrochemical detection (HPLC–ED). Animals from the experimental and control groups were decapitated under deep anesthesia 2, 7, 14 and 56 days after injury ($n = 6$–10 for each time point). The brains were quickly removed and the cortices dissected. Tissue samples were immediately frozen in liquid nitrogen and stored at −80°C until quantitative measurement of the brain catecholamines. These samples were weighed and initially added to 1 ml per 100 mg of 0.1 M perchloric acid containing 0.1 mM of sodium pyrosulfite and 0.02 mM of ethylenodiamine tetra-acetic acid disodium salt (EDTA 2Na). The mixture was then homogenized with an ultrasonic cell disruptor at 0°C for 30 sec and centrifuged at 12,000 rpm for 20 min at 0°C. The supernatant was filtered through a 0.45 μm centrifugal filter at 12,000 rpm for 15 mins at 0°C to separate the insoluble residue. A portion of the supernatant was then further centrifuged at 20,000 rpm for 2 min and an aliquot of the supernatant was injected into the HPLC–ED system. The HPLC–ED system was similar to that described by Takeda *et al.*[26]. The mobile phase was prepared with 50 mM disodium hydrogenphosphate 12-water, 50 mM citric acid, 4.4 mM sodium l-heptanesulphonate, 0.1 mM EDTA 2Na, 7.7% methanol and 3.1% asetonitrile, pH 3.0. This was run over a MCM C_{18} 5 μm column (150 mm × 4.6 mm i.d.) with a flow rate of 0.9 ml min^{-1} at 23°C. The conditioning cell was set at 350 mV and the analytical cell (dual coulometric working electrodes) at 80 mV and 350 mV.

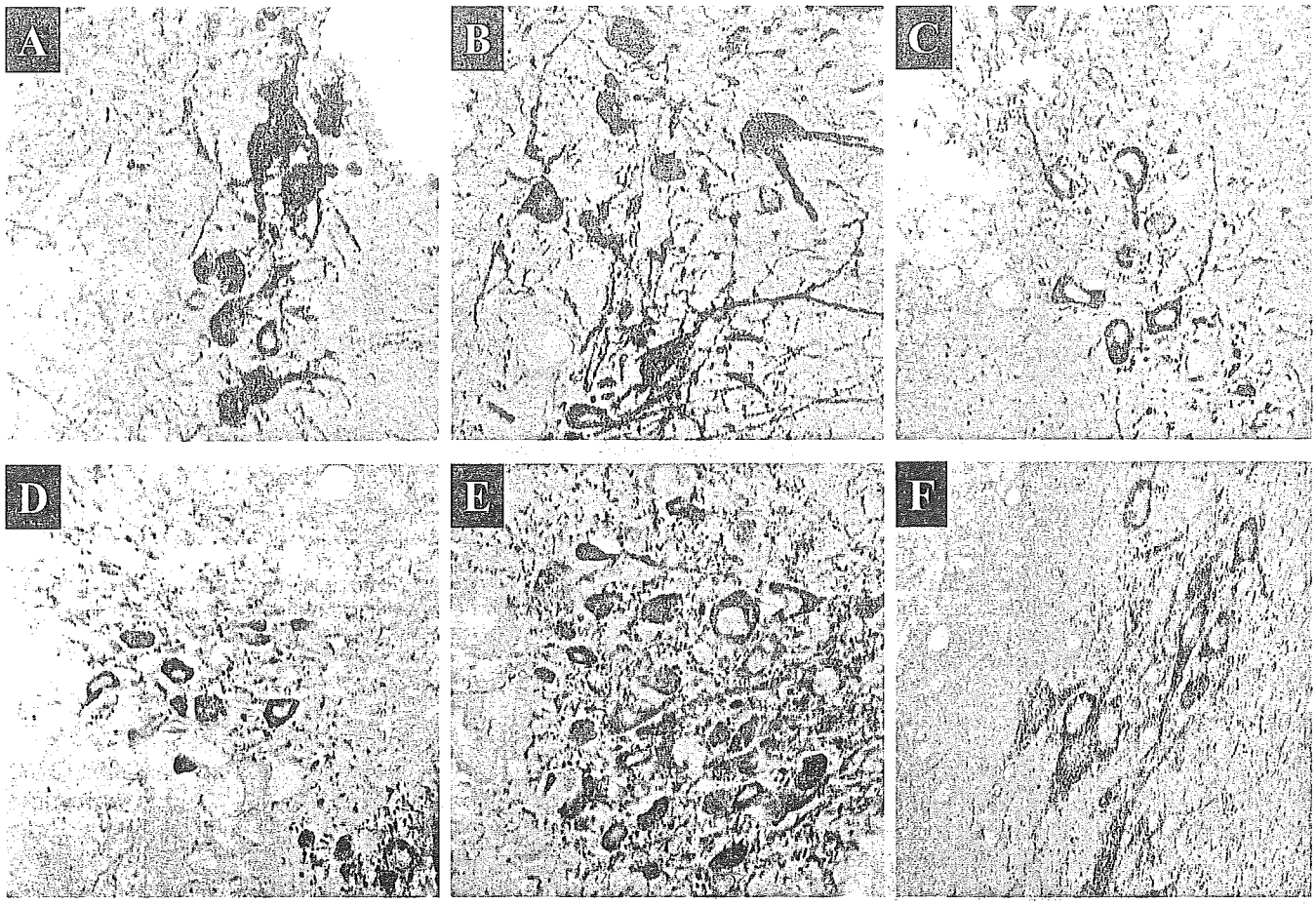

Figure 1: Photomicrographs of locus coeruleus (LC) immunostained with anti-dopamine-β-hydroxylase (DBH) in **A:** control animal, **B:** 24 h after injury, **C:** one week after injury, **D:** two weeks after injury, **E:** four weeks after injury, **F:** eight weeks after injury. Shrinkage of LC neurons immunostained with DBH was observed one and two weeks after injury. Four and eight weeks after injury, LC neurons were the same size as those of control animals

NE turnover was defined as the ratio of MHPG to NE levels[27,28]. For each of the experimental animals, this ratio was displayed as a percentage of the average for control animals, and expressed as mean ± SEM values. Statistical differences in the NE turnover between the experimental and control groups were assessed by ANOVA with the Newman–Keuls test for intergroup multiple comparisons. For this analysis, NE turnover values from both sides of the cortices were averaged together, and differences between the sides at each time point were analyzed with a *t*-test. A *p*-value of 0.05 or less was regarded as statistically significant.

RESULTS

Seventy-seven rats underwent the impact–acceleration brain injury. The mortality immediately after the injury was 19.5% (15/77). Post-traumatic seizure was observed in 39 (62.8%) of the surviving animals. Recovery from anesthesia took longer for injured animals than for control animals. Spontaneous motility in the survivors was reduced after recovery from anesthesia. Body weight was reduced to 86.6 ± 2.52% one week after injury and recovered to 100.7 ± 9.16% in four weeks. Subarachnoid and intraventricular hemorrhages were frequently observed, but skull fracture and contusion did not occur in any animals throughout the experiment. Immunohistochemistry for anti-68kD-neurofilament showed extensive axonal injury particularly in the ventral and central brain stem one or two days after injury.

Immunohistochemistry for DBH showed that the size of the LC neurons tended to increase initially one day after injury but thereafter decreased in size. One week after injury, LC neurons immunostained with DBH were noticeably smaller than those of control animals. No significant loss of cells was observed in the LC, and four and eight weeks after injury, the LC neurons were the same size as those of control animals (*Figure 1*). The axons of the LC neurons and the dorsal catecholamine bundles, the projection pathway of noradrenergic

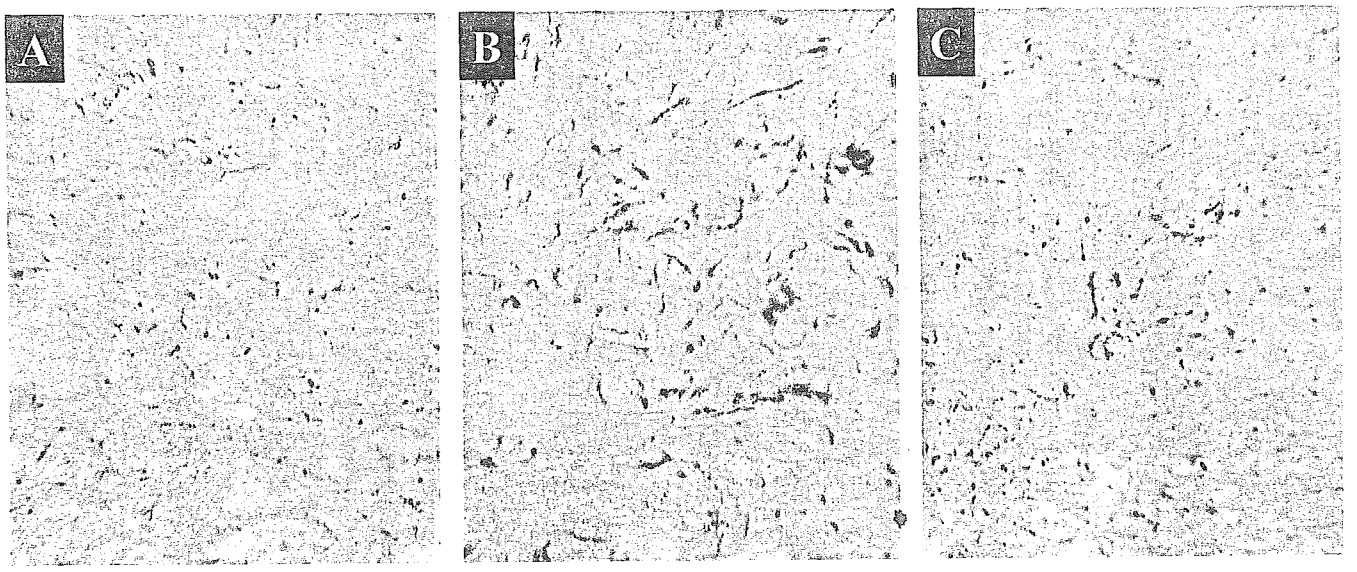

Figure 2: Photomicrographs of dorsal catecholamine bundles immunostained with anti-dopamine-β-hydroxylase in **A:** control animal, **B:** 24 h after injury, **C:** one week after injury. The axons of the dorsal catecholamine bundles were swollen 24 h after injury but the swelling had dwindled in one week

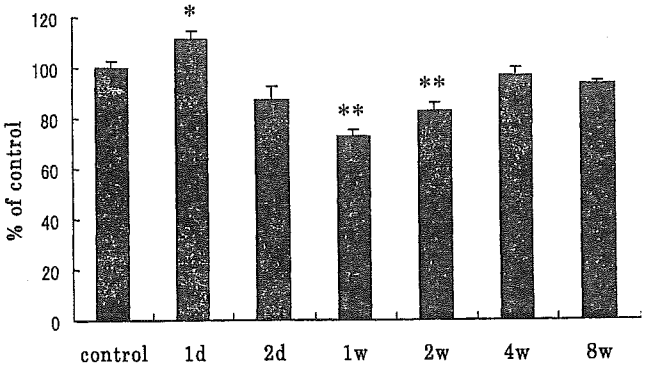

Figure 3: Cross-sectional area of locus coeruleus (LC) neurons immunostained with anti-dopamine-β-hydroxylase. Data are shown as a percentage of control animals. The values are means ± SEM, $*p < 0.05$, $**p < 0.01$

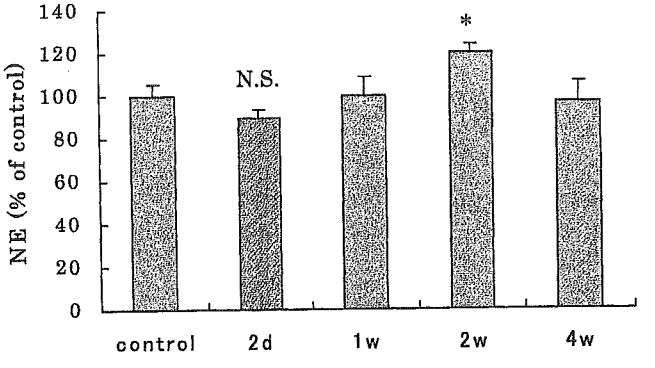

Figure 4: Total amount of norepinephrine (NE) in the cortex. Data are shown as a percentage of control animals. The values are means ± SEM. * indicates $p < 0.05$

neurons, were swollen 24 h and 48 h after injury but the swelling had dwindled in seven days (*Figure 2*). Quantitative image analysis confirmed these findings. The size of the LC neurons immunostained with DBH increased by 11.2 ± 3.58% ($p < 0.05$ compared to control) 24 h after injury. The mean size of the LC neurons immunostained with DBH decreased to 72.9 ± 2.07% ($p < 0.01$ compared to control) seven days after injury and to 82.4 ± 3.71% ($p < 0.01$ compared to control) 14 days after injury. Four and eight weeks after injury, the size had returned to near control value (*Figure 3*).

Tissue levels of NE and MHPG were measured with HPLC–ED. Total amount of NE in the cortex was not reduced during the experimental period, and two weeks after injury it had significantly increased ($p < 0.05$ compared to control) (*Figure 4*). Norepinephrine turnover, defined as the ratio of MHPG to NE levels and shown as a percentage of that of control animals, had not changed in the cortex two days after injury, but decreased significantly one, two and eight weeks after injury ($p < 0.01$ compared to control). One week after injury, NE turnover was 22.6 ± 3.38% of control value, and then gradually increased but remained significantly low even eight weeks after injury. No significant difference in NE turnover was found between the cerebral cortices on either side throughout the experiment (*Figure 5*).

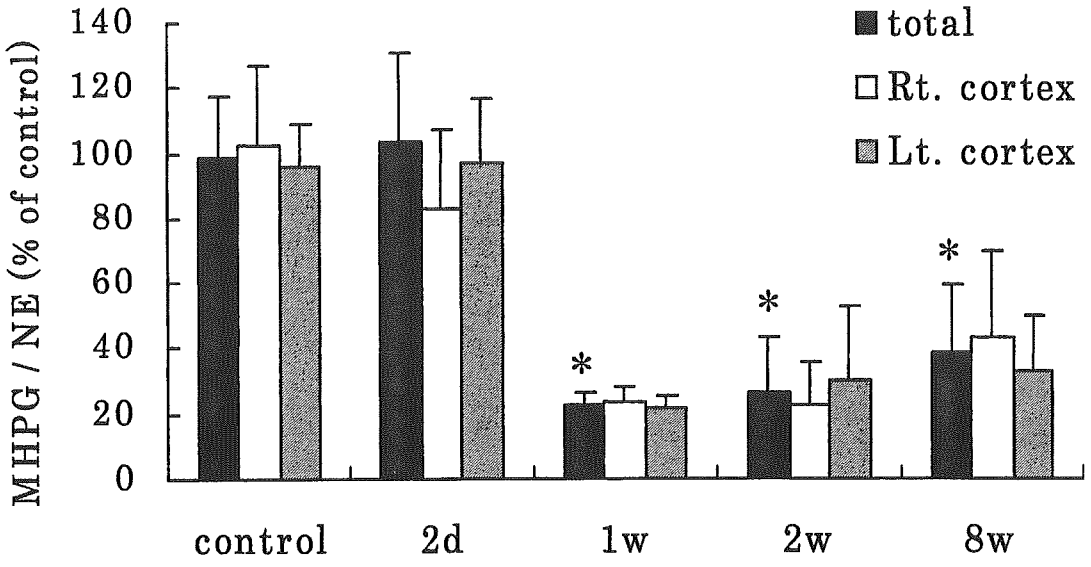

Figure 5: Norepinephrine (NE) turnover displayed as a percentage of control animals. NE turnover is defined as the ratio of 3-methoxy-4-hydroxyphenylglycol (MHPG) to NE levels. Data are shown as a percentage of control animals. The values are means ± SEM. * indicates $p < 0.01$

DISCUSSION

Marmarou *et al.*[24,25] described an experimental model capable of producing diffuse brain injury in the rodent. As the original method when used by us resulted in high mortality and high frequency of skull fracture, we modified a few points for our study. We used a metallic disc 20 mm in diameter and the weight was dropped from a height of 1.5 m. Immediate mortality was about 20%. Histological examination revealed typical signs of diffuse axonal damage particularly in the brainstem without apparent contusional damage underneath the disc.

We examined the central noradrenergic system following impact–acceleration brain injury. The locus coeruleus is a nucleus located in the tegmentum of the upper pons and consists mainly of pigmented neurons which contain norepinephrine. The noradrenergic pathways originating from the LC influence neural activities in many cortical regions of the brain and also distribute to subcortical structures, including the hypothalamus, hippocampus and cerebellar cortex[1–8]. Previous studies have suggested important roles for norepinephrine in the functional recovery after focal traumatic brain injury. Central norepinephrine concentration or its turnover decreased in the early phase after brain injury produced by either weight drop or cortical impact[13,19,22]. Intraventricular administration of norepinephrine could improve motor function after unilateral sensorimotor cortex ablation[15]. Drugs with an antagonistic effect on alpha 1 NE receptors, including haloperidol and prazosin, when administered early after a traumatic unilateral focal contusion in the sensorimotor cortex, retarded locomotor recovery[17,29]. Pre-treatment with the noradrenergic neurotoxin DSP-4 significantly retarded motor recovery in animals after unilateral sensorimotor cortex ablation[30]. Administration of L-threo-3,4-dihydroxyphenylserine, a precursor of NE, with benserazide, a peripheral aromatic amino acid decarboxylase inhibitor, promoted the recovery of locomotor function after unilateral sensorimotor cortex ablation injury[31].

Our study demonstrated the shrinkage of LC neurons in a diffuse brain injury model. The size of the LC neurons initially tended to increase by about 11% 24 h after injury, and the axons of noradrenergic neurons were swollen 24 h and 48 h after injury. These findings suggest that focal impairment of anterograde axonal transport due to diffuse brain injury induced initial cellular swelling of the LC neurons, but they decreased in size by about 27% seven days after injury but they returned to control value four and eight weeks after injury. Our impact–acceleration brain injury caused the initial swelling and following shrinkage of the LC neurons, but they recovered spontaneously within four weeks. LC neurons are known to have a strong regenerative response[32–35]. Administration of noradrenergic neurotoxin DSP-4 induced the initial cell loss in the LC and enhanced the sprouting from surviving neurons[35]. It is possible that these regenerative reactions were also induced in our model.

On the other hand, Carbary *et al.*[36] reported that no discernible qualitative differences were found between control and experimental animals in the intensity of immunostaining for either tyrosine or dopamine-β-hydroxylase in the ipsilateral LC 24 h or seven days after moderate fluid percussion injury. The biosynthesis of NE in the LC might not be affected by experimental moderate focal brain injury. Arakawa *et al.*[37] reported that changed EEG and LC neuronal activities recovered to pre-injury levels within 1 h after diffuse brain injury.

Their impact–acceleration injury model was produced with a 400 g weight dropped from a height of 1 m and all animals survived the impact–acceleration injury. Differences in the type and severity of injury may well be responsible for differences in cellular reaction.

Besides morphologic alterations in the LC neurons, the changes in NE metabolism are also related to disturbance of cortical functions[38–40]. We measured the tissue concentrations of NE and MHPG and calculated the ratio of MHPG to NE to reflect NE turnover[27,28]. With focal brain contusion, NE turnover was either eliminated or reduced bilaterally by 45%–92% in the cerebral cortex, hypothalamus, cerebellum, LC and medulla 24 h after injury[13]. With unilateral cerebral contusion, NE turnover initially and briefly increased 30 min after injury followed by bilateral widespread depression 6–24 h after injury[41]. In our study, NE turnover had not changed significantly in the cortex 48 h after injury, but had decreased significantly one week after injury. Although it was not examined whether NE turnover was affected in the chronic phase of the injury in the previous reports, we found that it remained at a very low level even eight weeks after injury. We did not observe any initial changes in NE turnover but our data showed prolonged depression of NE turnover in the chronic phase. The different nature of the experimental model and severity of injury may explain the differences in NE turnover. Whether NE turnover continued to decrease in the focal injury model is not clear. Two possible mechanisms might be involved in the prolonged impairment in NE turnover, loss of NE fibers projecting from the LC neurons or depression of NE synaptic activity. Although our study demonstrated that the LC neurons were affected in the early phase as was shown by the reduction in size one to two weeks after injury, they recovered their size four to eight weeks after injury. Damaged NE fibers are thus likely to recover in the chronic phase. Indeed, the total content of NE in the cortex was not reduced but rather increased two weeks after injury. However, NE turnover which remained affected one to two weeks after injury did not recover in the chronic phase (eight weeks after injury) either, which indicates prolonged depression of cortical synaptic activity. Details of the mode of impairment of this important neurotransmission system are not clear at present. Further clarification of the pathophysiology of the central noradrenergic system is considered indispensable for the development of optimal management of patients with diffuse brain injury in order to facilitate neuropsychological recovery.

REFERENCES

1 Olsen L, Fuxe K. On the projections from the locus coeruleus noradrenaline neurons: The cerebellar innervation. *Brain Res* 1971; **28**: 165–171

2 Kobayashi RM, Palkovits M, Kopin IJ, Jacobowitz DM. Biochemical mapping of noradrenergic nerve arising from rat locus coeruleus. *Brain Res* 1974; **77**: 269–279

3 Crow TJ, Deakin JFW, File SE, Longden A, Wendlandt S. The locus coeruleus noradrenergic system – evidence against a role in attention, habituation anxiety and motor activity. *Brain Res* 1978; **155**: 249–261

4 Foote SL, Bloom FE, Aston-Jones G. Nucleus locus coeruleus: New evidence of anatomical and physiological specificity. *Physiol Rev* 1983; **63**: 844–914

5 Saper CB. Function of the locus coeruleus. *Trends Neurosci Lett* 1987; **10**: 343–344

6 Sakaguchi T, Nakamura S. The mode of projections of single locus coeruleus neurons to the cerebral cortex in rats. *Neuroscience* 1987; **20**: 221–230

7 Fritschy JM, Grzanna R. Distribution of locus coeruleus axons within the rat brainstem demonstrated by Phaseolus vulgaris leucoagglutinin anterograde tracing in combination with dopamine-beta-hydroxylase immunofluorescence. *J Comp Neurol* 1990; **291**: 616–631

8 Petrov T, Krukoff TL, Jhamandas JH. Branching projections of catecholaminergic brainstem neurons to the paraventricular hypothalamic nucleus and the central nucleus of the amygdala in the rat. *Brain Res* 1993; **609**: 81–92

9 Huger F, Patrick G. Effect of concussive head injury on central catecholamine levels and synthesis-rates in rat brain regions. *J Neurochem* 1979; **33**: 89–95

10 Levin BE. Alterations of norepinephrine metabolism in rat locus coeruleus neurons in response to axonal injury. *Brain Res* 1983; **289**: 205–214

11 Globus MYT, Busto R, Dietrich WD, Martinez E, Valdés I, Ginsberg MD. Direct evidence for acute and massive norepinephrine release in the hippocampus during transient ischemia. *J Cereb Blood Flow Metab* 1989; **9**: 892–896

12 Sutton RL, Krobert KA. Acute changes in cortical noradrenaline levels of the anesthetized rat following cortical contusion: A microdialysis study. *J Neurotrauma* 1993; **10**: S181

13 Dunn-Meynell A, Pan S, Levin BE. Focal traumatic brain injury causes widespread reductions in rat brain norepinephrine turnover from 6 to 24 h. *Brain Res* 1994; **660**: 88–95

14 Levin BE, Pan S, Dunn-Meynell A. Chronic alterations in rat brain α-adrenoceptors following traumatic brain injury. *Restor Neurol Neurosci* 1994; **7**: 5–12

15 Boyeson MG, Feeney DM. Intraventricular norepinephrine facilitates motor recovery following sensorimotor cortex injury. *Pharmacol Biochem Behav* 1990; **35**: 497–501

16 Goldstein LB, Davis JN. Post-lesion practice and amphetamine-facilitated recovery of beam-walking in the rat. *Restor Neurol Neurosci* 1990; **1**: 311–314

17 Feeney DM, Westerberg VS. Norepinephrine and brain damage: Alpha noradrenergic pharmacology alters functional recovery after cortical trauma. *Can J Psychol* 1990; **44**: 233–252

18 Goldstein LB, Coviello A, Miller GD, Davis JN. Norepinephrine depletion impairs motor recovery following sensorimotor cortex injury in the rat. *Restor Neurol Neurosci* 1991; **3**: 41–47

19 Krobert KA, Sutton RL, Feeney DM. Spontaneous and amphetamine-evoked release of cerebellar noradrenaline after sensorimotor cortex contusion: An *in vivo* microdialysis study in the awake rat. *J Neurochem* 1994; **62**: 2233–2240

20 Sutton RL, Feeney DM. α-Noradrenergic agonists and antagonists affect recovery and maintenance of beam-walking ability after sensorimotor cortex ablation in the rat. *Restor Neurol Neurosci* 1992; **4**: 1–11

21 Prasad MR, Dose JM, Dhillon HS, Carbary T, Kraemer PJ. Amphetamine affects the behavioral outcome of lateral fluid percussion brain injury in the rat. *Restor Neurol Neurosci* 1995; **9**: 65–75

22 Prasad MR, Ramaiah C, Mcintosh TK, Dempsey RJ, Hipkens S, Yurek D. Regional levels of lactate and norepinephrine after experimental brain injury. *J Neurochem* 1994; **63**: 1086–1094

23 Levin BE, Brown KL, Pawar G, Dunn-Meynell A. Widespread and lateralized effects of acute traumatic brain injury on norepinephrine turnover in the rat brain. *Brain Res* 1995; **674**: 307–313

24 Marmarou A, Foda MAAE, van den Brink W, Campbell J, Kita H, Demetriadou K. A new model of diffuse brain injury in rats. Part 1: Pathophysiology and biomechanics. *J Neurosurg* 1994; **80**: 291–300

25 Foda MAAE, Marmarou A. A new model of diffuse brain injury in

rats, Part II: Morphological characterization. *J Neurosurg* 1994; **80**: 301–313
26 Takeda H, Matsumiya T, Shibuya T. Detection and identification modes for the highly sensitive and simultaneous determination of various biogenic amines by coulometric high-performance liquid chromatography. *J Chromatogr* 1990; **515**: 265–278
27 Schanberg SM, Schildkraut JJ, Breese GR, Kopin IJ. Metabolism of normetanerphrine-H3 in rat brain identification of conjugated 3-methoxy-4-hydroxyphenylglycol as the major metabolite. *Biochem Pharmacol* 1968; **17**: 247–254
28 Westerink BHC. Determination of normetanephrine, 3,4-dihydroxyphenylethyleneglycol (free and total), and 3-methoxy-4-hydroxyphenylethyleneglycol (free and total) in rat brain by high-performance liquid chromatography with electrochemical detection and effects of drugs on regional concentrations. *J Neurochem* 1984; **42**: 934–942
29 Dunn-Meynell AA, Yarlagadda Y, Levin BE. α1-adrenoceptor blockade increases behavioral deficits in traumatic brain injury. *J Neurotrauma* 1997; **14**: 43–52
30 Boyeson MG, Callister TR, Cavazos JE. Biochemical and behavioral effects of a sensorimotor cortex injury in rats pretreated with the noradrenergic neurotoxin DSP-4. *Behav Neurosci* 1992; **106**: 964–973
31 Kikuchi K, Nishino K, Ohyu H. Increasing CNS norepinephrine levels by the precursor L-DOPS facilitates beam-walking recovery after sensorimotor cortex ablation in rats. *Brain Res* 2000; **860**: 130–135
32 Stenevi U, Björklund A, Moore RY. Growth of intact adrenergic axons in the denervated lateral geniculate body. *Exp Neurol* 1972; **35**: 290–299
33 Nakai K, Jonsson G, Kasamatsu T. Norepinephrinergic reinnervation of cat occipital cortex following localized lesion with 6-hydroxydopamine. *Neurosci Res* 1987; **4**: 433–453
34 Nakai K. Regenerative catecholamine-containing terminals in kitten visual cortex: An ultrastructual study. *Neurosci Res* 1987; **4**: 475–485
35 Fritschy JM, Grazanna R. Restoration of ascending noradrenergic projections by residual locus coeruleus neurons: Compensatory response to neurotoxin-induced cell death in the adult rat brain. *J Comp Neurol* 1992; **321**: 421–441
36 Carbary T, Dhillon HS, Scheff SW, Prasad RM. Immunohistochemistry of tyrosine and dopamine-β-hydroxylases after experimental brain injury in the rat. *Neurosci Res Comm* 1996; **18**: 79–85
37 Arakawa S, Nakamura S, Kawashima N, Nishiike S, Okuyama S. Antagonizing effects of VA-045 on reduced activity of rat locus coeruleus neurons following head injury or intravenous injection of clonidine. *Life Sci* 1995; **57**: 1803–1810
38 Foote SL, Aston-Jones G, Bloom FE. Impulse activity of locus coeruleus neurons in awake rats and monkeys is a function of sensory stimulation and arousal. *Proc Natl Acad Sci USA* 1980; **77**: 3033–3037
39 Aston-Jones G, Bloom FE. Norepinephrine-containing locus coeruleus neurons in behaving rats exhibited pronounced responses to non-noxious environmental stimuli. *J Neurosci* 1981; **1**: 887–900
40 Berridge CW, Page ME, Valentino RJ, *et al.* Effect of locus coeruleus inactivation on electroencephalographic activity in neocortex and hippocampus. *Neuroscience* 1993; **55**: 381–393
41 Dunn-Meynell AA, Hassanain M, Levin BE. Norepinephrine and traumatic brain injury: A possible role in post-traumatic edema. *Brain Res* 1998; **800**: 245–252